Conformational analysis of cyclohexyl hydroperoxide by rotational spectroscopy.

Pablo Pinacho,*[a] Wenhao Sun,[a] Daniel A. Obenchain,[b] and Melanie Schnell[a,c]
a) Deutsches Elektronen-Synchrotron DESY, Notkestr. 85, 22607 Hamburg, Germany.
b) Institut für Physikalische Chemie, Universität Göttingen, Tammannstr. 6, 37077 Göttingen, Germany
c) Christian-Albrechts-Universität zu Kiel, Institut für Physikalische Chemie, Max-Eyth-Str. 1, 24118 Kiel, Germany.

Keywords: Rotational spectroscopy, gas-phase spectroscopy, molecular structure, conformational relaxation

Abstract: Cyclohexyl hydroperoxide was observed in the gas phase using a supersonic expansion coupled with broadband chirped-pulse Fourier transform microwave spectroscopy. Cyclohexyl hydroperoxide is a simple but important organic peroxide due to its rather high stability in solution and because of its applications in polymer industry. Furthermore, it is one of the products of the oxidation process of cyclohexane. We detected this molecule in the spectrum of a complex non-commercial sample containing many molecular species from the oxidation of cyclohexane. The peroxy group O-O-H gives flexibility to the molecule and results in different stable conformations. Each of the conformations presents two equivalent forms due to the high symmetry of cyclohexane. From the dataset of rotational constants observed, we determined a partial effective structure for cyclohexyl hydroperoxide and compared it with other peroxides studied in the gas phase.

Introduction

Peroxides (R-O-O-R'), either organic or inorganic, are one of the most important family of compounds for chemistry.[1] Due to the rather weak oxygen-oxygen (-O-O-) bond, they are highly reactive and decompose spontaneously to more stable compounds.[2] If stored under appropriate conditions, hydrogen peroxide (H_2O_2) has a long shelf life. However, concentrated solutions of H_2O_2 in the presence of certain metals can undergo explosive decomposition. Both organic and inorganic peroxides are hazardous substances, which have to be handled carefully. They are highly flammable, and if mixed with reducing agents will react violently. Despite their hazards, peroxides are commonly found in research and industry due to their numerous applications. Organic peroxides are important as radical initiators in the manufacture of polymers[3,4] and oxidation processes.[5] H_2O_2 and other organic peroxides play a key role in the mechanism of oxidation of chemical species in the atmosphere.[6-8] In addition to their interest in the polymer industry and atmospheric processes, the peroxides have other uses for food manufacture, treatment of diseases,[9] or in biological processes.[10]

One of the simplest and most important organic peroxides is cyclohexyl hydroperoxide (CHHP), in which the hydroperoxide is attached to a cyclohexyl ring (Figure 1). Since the 1950s, CHHP is known to be one of the products of the oxidation of cyclohexane.[11] Like most peroxides, CHHP is highly reactive and decomposes easily, but it presents a striking stability in solution compared to other peroxides.[11,12] CHHP has been described to be an extremely good catalyst in polymerization reactions.[11] In the liquid phase, the reactivity of CHHP and its stability are influenced by the solvent.[11] The first step towards a better understanding of the mechanism of action of CHHP and other peroxides is to have an accurate characterization of their inherent structures in the gas phase. However, there is little knowledge about the structure and interactions of these types of molecules in isolated conditions.

Several peroxides (including H_2O_2, CH_3-O-O-CH_3, Me_3-C-O-O-C-Me_3, CF_3-O-O-H, or CF_3-O-O-Cl) have been studied in the gas phase by gas electron diffraction (GED), providing accurate structures.[1,13-16] Another powerful tool to determine the structures of molecules and complexes in an isolated environment, is high-resolution rotational spectroscopy coupled with supersonic expansions.[17] Nowadays, most of the characterizations are done using broadband chirped-pulse Fourier transform microwave spectrometers,[18] which allow for fast experiments keeping the high resolution of rotational spectroscopy.[19] So far, the characterization by rotational spectroscopy is limited to H_2O_2 and a few other peroxides (such as Cl-O-O-Cl, HC(O)O-O-O-H, or CF_3-O-O-F).[1,20-23]

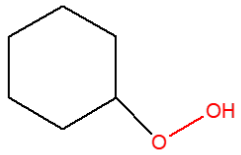

Figure 1. The chemical structure of cyclohexyl hydroperoxide (CHHP).

In this work, we report the detection of CHHP using rotational spectroscopy in the gas phase. CHHP was found in non-commercial samples containing products from the oxidation of cyclohexane. We performed quantum-chemical computations to guide the analysis of the spectrum, predict the molecular structures, and model the intramolecular dynamics of CHHP.

Experimental and theoretical methods

We used a non-commercial sample resulting from the (partial) oxidation of cyclohexane to investigate cyclohexyl hydroperoxide. The main component of this sample is cyclohexane, which cannot be detected by microwave spectroscopy due to the lack of a dipole moment. Minor amounts of other components, such as cyclohexanol, are also present (Figure 2). In this work, we

are focusing on CHHP, while the spectroscopic identification of the other components will be addressed in a future publication.

The sample was analyzed using chirped-pulse Fourier transform microwave (CP-FTMW) spectroscopy.[18] The rotational spectrum was recorded in the 18-26 GHz region using our K-band spectrometer.[24] The sample is a liquid at standard conditions. It was held in a metallic reservoir with some glass wool and heated to *ca*. 45 °C to increase the vapor pressure. The vapor was diluted in neon as a carrier gas at about 2 bars of backing pressure. The mixture was introduced into the vacuum chamber of the K-band spectrometer through a small diameter nozzle (1 mm), generating a pulsed supersonic expansion.

The K-band instrument is based on a combination of the segmented approach[25] and a multi-train setup.[26] The spectrum between 18 and 26 GHz is divided into segments of 800 MHz each, which are concatenated in a pulse train to produce the 8 GHz bandwidth. Such pulse trains are replicated to obtain a multi-train, which is applied on each supersonic expansion pulse. Three pulse trains are applied per gas pulse, which gives an effective repetition rate of 30 Hz combined with a repetition rate of 10 Hz for the gas pulses. More details about the instrument can be found elsewhere.[24] The microwave pulse is generated by an arbitrary waveform generator, up-converted, amplified, and introduced into the vacuum chamber by a horn antenna. The microwave pulse polarizes the molecular ensemble. The signal in form of a free-induction decay (FID) is collected in the time domain as the free-induction decay of the molecular ensemble, down-converted, averaged in the time domain, and converted into the frequency domain by the application of the Fourier transformation. A total of 2.0 million FIDs were recorded. The spectrum is characterized by a resolution of around 100 kHz and accuracy in frequency measurement better than 15 kHz. An excerpt of the recorded spectrum is presented in Figure 2 showing some of the transitions detected for cyclohexyl hydroperoxide together with some nearby transitions from cyclohexanol.

A conformational search was performed to obtain the possible minimum structures for CHHP, using the tight-binding method GFN-xTB from the CREST program.[27] The geometries were optimized at the B3LYP-D3(BJ)/def2-TZVP[28-30] level of theory using the ORCA software.[31] Energy scans for certain motions were also performed at B3LYP-D3(BJ)/def2-TZVP using ORCA to compute their barrier heights. In addition, frequency calculations were done at the same level of theory to confirm that all the structures were real minima, to obtain the zero-point corrected relative energies, and to obtain the theoretical values of the centrifugal distortion constants. Those frequency calculations were performed using both Orca and Gaussian.[32] The program PGOPHER[33] developed by Colin M. Western was used to plot the experimental spectrum, simulate the rotational transitions based on the theoretical and experimental parameters, and provide initial fits. Final fits were achieved by applying an *A*-reduction semirigid rotor Hamiltonian in the I^r representation[17,34] using the CALPGM suite,[35] obtained from the PROSPE webpage.[36]

Finally, we also performed non-covalent interactions (NCI) calculations to identify and visualize the weak intramolecular interactions.[37,38] To determine the type and strength of non-covalent forces, the sign and value of the Hessian of the electron density are evaluated and plotted.

Results and discussion

Conformational landscape and microwave spectrum

Three low-energy conformers of CHHP were predicted by the combination of CREST with further optimization at the B3LP-D3(BJ)/def2-TZVP level of theory. Some additional structures were predicted, but all of their relative energies are higher than 13 kJ/mol after the optimization. The three low-energy structures with different heavy-atom backbone conformations were found to be within only 3 kJ/mol of relative energy (Table 1). In the three conformers, the cyclohexane ring is in the most stable chair form (Figure 3). The conformers can be differentiated by the values of two dihedral angles; τ, C_1-C_2-C_3-C_4, and φ, C_2-C_1-O_7-O_8, which characterize the cyclohexane backbone and the hydroperoxide orientation, respectively. CHHP 1 and CHHP 3 have the same value for the τ dihedral angle, while this parameter has the opposite sign for CHHP 2, reflecting the ring flipping of cyclohexane in that conformation (Figure 3).[39] The φ dihedral angle takes different values for each of the conformers, showing the flexibility of the O-O-H group.

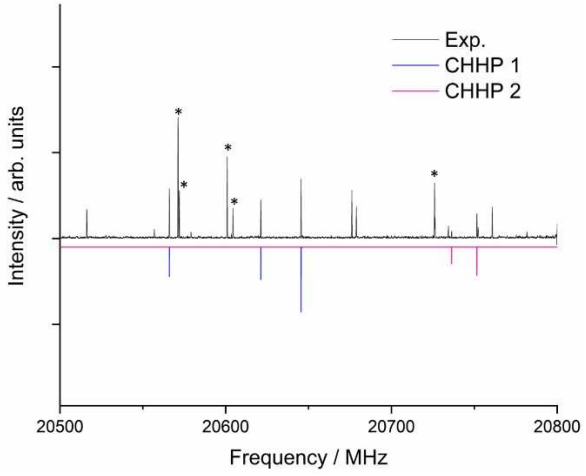

Figure 2. Excerpt of the rotational spectrum of the sample measured in this work. The top trace shows the experimental spectrum. The bottom trace is the simulation for CHHP 1 and CHHP 2 based on the fitted parameters. The marked lines (*) belong to cyclohexanol.

The experimental spectrum was visualized using PGOPHER and compared against simulations for the rotational transitions based on the predicted parameters. Although the spectrum is rather weak, it was possible to detect different species. After several fitting-plotting iterations, two sets of rotational constants could be obtained, which were later refined using the CALPGM suite. CALPGM is composed of two programs, SPFIT and SPCAT, which allow for fitting the rotational parameters and simulating the microwave spectrum iteratively.[35] Due to the low intensity of the transitions, no lines belonging to

^{13}C isotopologues were observed in natural abundance, and thus, we could not derive the experimental structure of CHHP. The assignment of the observed species to theoretical structures relies on a good agreement with the predicted parameters. The rotational constants determined are presented in Table 1 and show an agreement between theory and experiment with a deviation of less than 1%. In the case of the quartic centrifugal distortion constants, there is also an excellent agreement between the theoretical values and those obtained from the fit. The large difference in the distortion constants between the conformers is accurately reproduced by the computations as well.

The first set of rotational constants can be assigned to CHHP 1, the global minimum. It could also be attributed to CHHP 1' (*vide infra*), however, the intensities of the experimental transitions agree better with the dipole-moment component values predicted for CHHP 1 than for CHHP 1' (Table S1 and Figure S1). The second set can be correlated to CHHP 2 or CHHP 2'. Based on the good agreement of the rotational constants and the dipole-moment components, we can identify it as CHHP 2, because of the small predicted value for the μ_a component of the electric dipole moment (Table S1), in agreement with the non-observation of *a*-type transitions in the spectrum. No rotational transitions that could correspond to CHHP 3 were observed although it should be present in the supersonic expansion based on its relative energy. The non-observation of CHHP 3 could be due to the overall rather low intensity of the spectrum. For CHHP 2, the second conformer in energy, only 32 rotational transitions were detected. Thus, it is possible that even though CHHP 3 is populated, we would not observe any rotational transitions belonging to this species due to the overall low number density. Another factor to consider is possible motions that result in relaxations, as described below. The observed frequencies for both CHHP 1 and CHHP 2 are collected at the end of the supplementary material.

Intramolecular motions

Most of the peroxides studied in the gas phase so far are symmetric with identical substituents at both oxygen atoms (R-O-O-R, with R being a substituent). In the case of CHHP, only one of the peroxy atoms is substituted, and the orientation of the O-O-H group breaks the symmetry, making it chiral. We can consider the cyclohexane ring as a static part on the time scale of our experiment and at the low temperatures in the supersonic jet due to the high barrier for chair-boat isomerization, with the much lighter O-O-H group resulting in different conformations (Figure 3). In addition, due to the high symmetry of the cyclohexane backbone, concerted rotations of the flexible O-O-H group connect pairs of enantiomers (Figure 4).

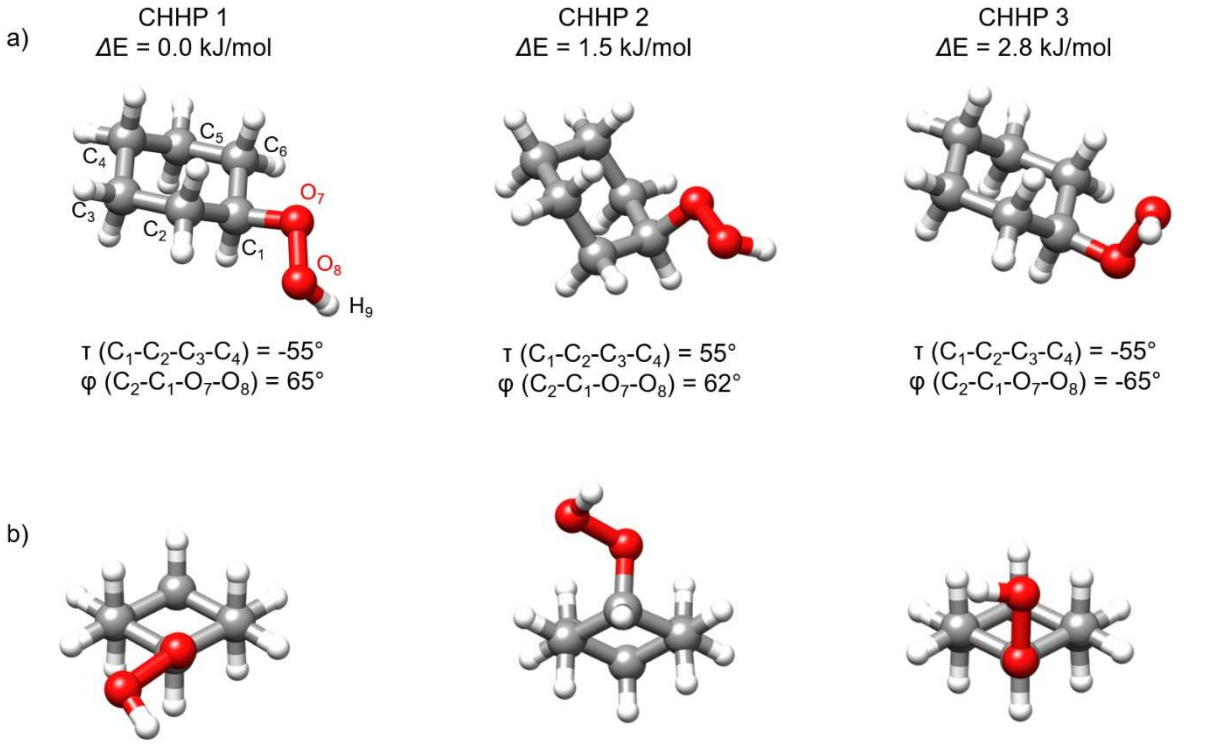

Figure 3. Three low-energy conformers of CHHP in a) side view and b) front view. The zero-point corrected relative energies are given at the B3LYP-D3(BJ)/def2-TZVP (black) and MP2/aug-cc-pVTZ (red) levels of theory for those three conformers. The values for the τ and φ dihedral angles are displayed to show the difference in the molecular structures.

Table 1. Experimental and theoretical parameters (B3LYP-D3(BJ)/def2-TZVP) for the lowest energy structures of CHHP.

	Experimental		Theoretical		
	CHHP 1	***CHHP 2***	***CHHP 1***	***CHHP 2***	***CHHP 3***
A / MHz[a]	3967.61978(53)[b]	3272.1609(37)	3985	3291	3660
B / MHz	1363.29303(31)	1619.7885(14)	1357	1609	1436
C / MHz	1091.97964(36)	1348.8634(13)	1089	1339	1204
Δ_J / kHz	0.0701(15)	0.354(13)	0.069[c]	0.354	0.103
Δ_{JK} / kHz	0.1059(46)	-1.139(85)	0.110	-1.149	0.080
Δ_K / kHz	0.615(21)	2.198(91)	0.597	2.304	0.687
δ_J / kHz	0.01789(64)	0.0306(43)	0.016	0.032	0.010
δ_K / kHz	0.189(22)	[0]	0.235	0.140	-0.066
μ_a / D	Y	N	-1.00	0.01	-1.36
μ_b / D	Y	Y	-0.52	0.84	1.37
μ_c / D	Y	Y	-1.44	-1.36	-0.22
n	105	32	-	-	-
σ / kHz	8.0	10.3	-	-	-
ΔE / kJ/mol	-	-	0.0	1.3	2.7
ΔE_{ZPE} / kJ/mol	-	-	0.0	1.5	2.8

[a] A, B, and C are the rotational constants in MHz. Δ_J, Δ_{JK}, Δ_K, δ_J, and δ_K are the quartic centrifugal distortion constants in kHz. μ_a, μ_b, and μ_c are the values of the electric dipole-moment components in Debye, the Y or N labels indicate whether such types of transitions have been observed or not. n is the number of fitted transitions. σ is the root-mean-square deviation of the fit. ΔE is the theoretical relative energy at the B3LYP-D3(BJ)/def2-TZVP level of theory in kJ/mol. ΔE_{ZPE} is the theoretical relative energy including the zero-point energy (ZPE) correction in kJ/mol. [b] Standard error in parentheses in units of the last digit. [c] The values of the quartic centrifugal distortion constants were predicted using Gaussian.

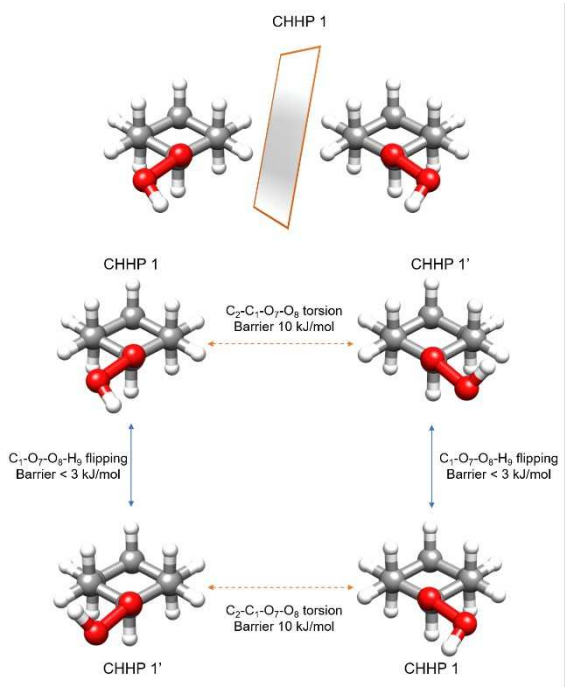

Figure 4. Schematic representation of the possible conversion pathways between the two mirror images of CHHP 1 through two concerted motions.

The torsion of the φ (C_2-C_1-O_7-O_8) coordinate connects CHHP 1 with CHHP 1', an almost isoenergetic structure, in which the only difference is the orientation of the H_9 atom (Figure 4). The calculations at the B3LYP-D3(BJ)/def2-TZVP level of theory predict CHHP 1' to be slightly lower in energy than CHHP 1, both considering the equilibrium and the zero-point corrected energy (ΔE = 0.3 kJ/mol, Table S1). Calculations at the MP2/aug-cc-pVTZ level of theory predict CHHP 1 to be lower in energy than CHHP 1' by 0.3 kJ/mol. According to the MP2 calculations, CHHP 2 is also isoenergetic with CHHP 1 (Table S1). The experimental intensities agree much better with the prediction of the dipole-moment components of CHHP 1. For this reason, we identified the experimental species as CHHP 1 and not CHHP 1'.

We performed scans of the motions in CHHP to obtain the energy barrier heights for the conversion paths (Figure 5). The conversion of CHHP 1' to CHHP 1 by the torsion of the φ dihedral angle is hindered by a rather high energy barrier of around 10 kJ/mol (≈ 850 cm^{-1}), however, there is a second motion that connects both structures (Figures 4 and 5). The flipping of the H_9 atom, which can be described by the change of the Φ (C_1-O_7-O_8-H_9) coordinate, converts CHHP1 to CHHP1' by a potential energy curve with a barrier of less than 3 kJ/mol (≈ 250 cm^{-1}). This barrier is low enough to allow for the relaxation of CHHP 1' into CHHP 1 by collisions with the carrier gas atoms. To complete the inversion of the CHHP 1 structure requires a concerted torsion of φ, followed by a flipping of the hydrogen atom, resulting in two structures that are mirror images of each other (Figures 4 and 5). Such concerted motions have been observed before in other molecular systems, evidenced by the presence of splitting in the experimental spectrum.[40,41] Despite the presence of two equivalent structures for CHHP 1, no splittings attributed to a tunneling effect have been observed, because of the barrier height of the torsion motion, which prevents to complete the inversion. The torsion of the φ (C_2-C_1-O_7-O_8) coordinate also connects CHHP 1 with CHHP 3 (Figure

5), across a high energy barrier of ≈19 kJ/mol (≈1600 cm^{-1}), preventing the possible relaxation of CHHP 3 into CHHP 1. To obtain a more complete picture of the landscape of CHHP 1 and CHHP 1', we investigated the two-dimensional potential energy surface corresponding to the φ torsion and Φ flipping (Figure 6). Additional views of the two-dimensional surface are provided in Figure S2.

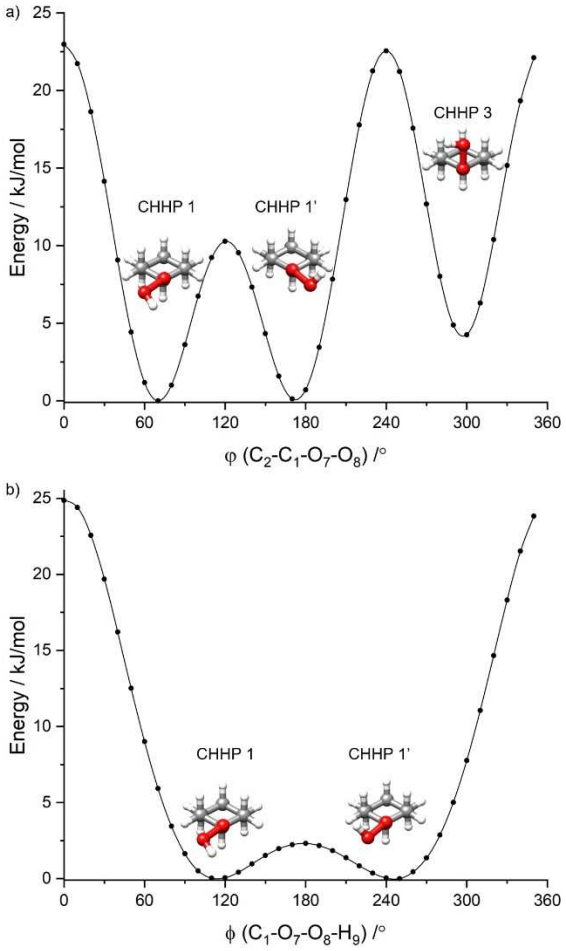

Figure 5. a) Potential energy curve for the φ (C_2-C_1-O_7-O_8) torsion showing the positions of CHHP 1, CHHP 1', and CHHP 3. b) Potential energy curve for the flipping of the hydrogen along the Φ (C_1-O_7-O_8-H_9) coordinate illustrating the positions of the conformers CHHP 1 and CHHP 1' (the structure depicted is the mirror image of CHHP 1 in panel a)). Both potential energy curves were calculated at the B3LYP-D3(BJ)/def2-TZVP level of theory scanning in steps of 10°.

Similar conclusions can be extracted for CHHP 2. This conformer also presents a mirror image structure. The inversion of the structure of CHHP 2 would require two concerted motions (Figure S3), passing by a structure with a different orientation for H_9, CHHP 2'. The change of the φ coordinate connects CHHP 2 with CHHP 2' and with another conformation, CHHP 4, which is much higher in energy by more than 14 kJ/mol (Figure S4). The conversion of CHHP 2' to CHHP 2 by the change of the C_2-C_1-O_7-O_8 dihedral angle passes by an energy barrier of around 10 kJ/mol (≈850 cm^{-1}), while the flipping of the H_9 atom requires overcoming a barrier of only 1.5 kJ/mol (≈120 cm^{-1}), explaining the non-observation of CHHP 2'.

As previously described, it is possible to connect the two pairs of equivalent forms by both motions, but the high barrier for the first torsion prevents to complete the inversion of the structure. The inversion of CHHP 3 is the simplest since it would only require one motion, hindered by a barrier of about 3 kJ/mol (Figures S5 and S6). In this case, we could expect to observe some splittings of the rotational transitions, however, conformer CHHP 3 was missing in our experimental spectrum (*vide supra*). The potential splitting could be another reason for this non-observation, because it further weakens the spectrum.

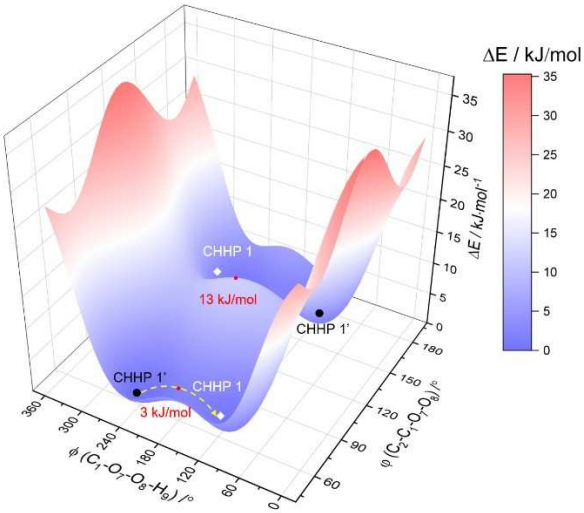

Figure 6. Potential energy surface for the conversion of CHHP 1 and CHHP 1' at the B3LYP-D3(BJ)/def2-TZVP level of theory. The surface was obtained by scanning the φ and Φ coordinates in steps of 10°, from 50° to 190°, and from 0° to 360° for φ and Φ, respectively. The conversion of CHHP1' into CHHP 1 is possible by the motion of the Φ coordinate passing by a low barrier of 3 kJ/mol (dashed yellow arrow).

It is worth comparing the system of CHHP with cyclohexanol, for which the gauche conformer presents two equivalent structures. The barrier for the inversion of the structure between two mirror images was determined to be about 4.5 kJ/mol (377 cm^{-1}) from the splittings observed experimentally.[42] In cyclohexanol, the rotation of the O-H group connects both equivalent structures, giving rise to tunneling splitting. The observed splittings of less than 0.5 MHz were associated with a difference between the two states $\Delta E_{0^+0^-}$ = 32.7(4) GHz and with a barrier for the motion of 4.5 kJ/mol. The splitting in the experimental spectrum is inversely related to the barrier height. The barrier for CHHP is predicted to be more than twice that of cyclohexanol, thus, the possible splittings for CHHP in the experimental region investigated (18 - 26 GHz) could be much smaller than those of cyclohexanol, not allowing us to resolve them, in agreement with our observations.

We compared the width of several lines of CHHP 1, CHHP 2, and the state 0^+ from cyclohexanol, which is also present in our experimental spectrum, as it is another product of the oxidation of cyclohexane. The rotational transitions of cyclohexanol are split, so the line widths of the transitions corresponding to the 0^+ state give a general indication of the width of "single" lines. The width was measured as the full-width half maximum

(FWHM) for four transitions for CHHP 1, CHHP 2, and cyclohexanol. The transitions were chosen to cover the full range of the spectrum. The results, collected in Table S2, show that the width of CHHP 1 and CHHP 2 (≈ 0.23 MHz) is very similar to that of cyclohexanol. Thus, if there is any spitting in the conformers of CHHP, it is smaller than the FWHM in our experiment.

Molecular structure

A critical parameter for peroxides is the Φ (R-O-O-R') dihedral angle, which is determined by the interplay between two factors: the attractive interaction between the lone pairs of both oxygen atoms and the repulsion between substituents.[1,13] In condensed phase studies of peroxides, this value is also largely affected by the intermolecular interactions, highlighting the need for accurate gas-phase structures for valuable comparisons.

We did not observe any isotopologues in natural abundance in the experimental spectrum and thus we could not determine the experimental substitution structure, r_s, limiting the structural information we can extract. However, we could determine a partial effective, r_0, structure using the STRFIT program, available from the PROSPE webpage.[36] For that, we performed a least-squares fit floating certain bond and angle values to reproduce the rotational constants in the vibrational ground state. The rest of the molecular parameters were kept fixed to the starting structure for the fit, taken from the calculations at the B3LYP-D3(BJ)/def2-TZVP level of theory. The number of parameters that can be fitted depends on the number of rotational constants available. For CHHP 1, we determined the O_7-O_8 bond distance together with the C_1-O_7-O_8 angle. For CHHP 2, we could only determine the O_7-O_8 distance, no other parameter could be obtained with enough confidence, resulting in an unsatisfactory fit. It is remarkable, that despite the O_7-O_8 bond distance being predicted to be the same for both conformers (1.45 Å), the fitted parameters diverge from CHHP 1 (1.471(4)) to CHHP 2 (1.418(8)). This could be due to the poorer r_0 fit achieved for CHHP 2, compared to CHHP 1 (Table S3). The r_0 rotational constants and coordinates are given in Tables S3-S5. The results of the r_0 structural parameters for CHHP are presented in Figure 7 together with the same parameters from equilibrium structures, and Table 2 shows a comparison with other peroxides. The O_7-O_8 distance of CHHP is similar to the distances from literature to peroxides. For the Φ dihedral angle of CHHP, it has an intermediate value between all the cases reported so far.

In CHHP, only one of the peroxy oxygen atoms presents a substitution group, so there is not a large repulsion effect between the substituents. We performed non-covalent interactions (NCI) calculations to plot and visualize the weak intramolecular interactions present in this molecule. Only two intramolecular forces were found, a repulsive one in the center of the cyclohexane ring, and an attractive C-H···O interaction of around 2.5 Å in both of the experimental conformations of CHHP. The result from the NCI analysis is represented in Figure 7.

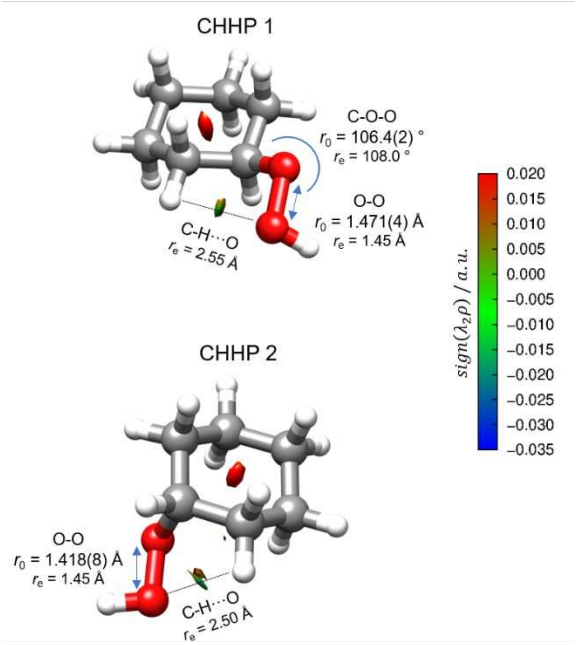

Figure 7. The partial effective structure, r_0, determined for the experimentally observed conformations of CHHP, together with the same parameters predicted from calculations at the B3LYP-D3(BJ)/def2-TZVP level of theory. The NCI is also plotted, showing an attractive C-H···O force. For the NCI illustration, an isosurface cut-off value of 0.5 was used. λ_2 is the second eigenvalue of the electron-density Hessian, and ρ is the electron density. A negative value of λ_2 indicates a strong attractive force, values of λ_2 close to 0 indicate the presence of weak attractive interaction, such as van der Waals forces. Positive values of λ_2 illustrate negative forces in the molecule.

Table 2. Molecular parameters for CHHP and other peroxides from literature. The values come from gas electron diffraction (GED), microwave (MW), or theoretical data.

Molecule	r O_7-O_8 /Å	Φ R-O_7-O_8-R' /°
H-O-O-H	1.467(5)[a]	120(2)[a]
	1.452(4)[b]	119.1(18)[b]
CH_3-O-O-CH_3[c]	1.457(12)	135(5)
CF_3-O-O-CF_3[d]	1.419(20)	123(4)
Cl-O-O-Cl[e]	1.426(2)	81.0(1)
F-O-O-F[f]	1.217(5)	87.5(5)
CHHP 1	1.471(4)[g]	111[h]
CHHP 2	1.418(8)[g]	108[h]

[a] From GED study, reference 13. [b] From MW study, reference [43]. [c] From GED study, reference 14. [d] From GED study, reference [44]. [e] From MW study, reference 21. [f] From MW study, reference [45], the atypical values were confirmed by GED study, reference [46]. [g] Present MW work, experimentally determined. [h] Present MW work, theoretically predicted.

Summary

We have observed two conformations of cyclohexyl hydroperoxide in the gas phase in a non-commercial sample containing multiple products from the oxidation of

cyclohexane. The spectrum was recorded with a recently built chirped-pulse broadband Fourier transform *K*-band spectrometer in the 18-26 GHz region. The rotation of the flexible O-O-H group of CHHP gives rise to three low-energy conformers. The rotation of that group also connects each conformer with its mirror image and another structure, almost isoenergetic, which only differs in the orientation of the hydrogen atom from the hydroperoxide group. We investigated the conversion pathways and the energy barriers for the motions of CHHP and found that there is a possible mechanism to convert CHHP 1' and CHHP 2' into CHHP 1 and CHHP 2, respectively. The second motion, which will complete the inversion, seems to pass by a rather high barrier, preventing the tunneling effect or making the tunneling splittings smaller than the resolution of the experimental set-up. No evidence of line splittings has been observed in the 18-26 GHz frequency range, which agrees with the predicted barriers for the complete inversion of the structure. Finally, despite the limited experimental dataset, we were able to apply a least-squares fit of selected structural parameters to reproduce the experimental rotational constants and obtain a partial effective structure. The bond distances and angles determined are in the same range as the theoretical calculations and are similar to other peroxides reported in the gas phase.

Acknowledgments

This work is supported via the collaborative linkage grant ''Extreme light for sensing and driving molecular chirality (ELCH)'', SFB1319, of the Deutsche Forschungsgemeinschaft. Parts of the computations were performed by using the European XFEL and DESY funded Maxwell computational resources operated at Deutsches Elektronen-Synchrotron DESY, Hamburg, Germany. P. P. would like to thank the Alexander von Humboldt Foundation for a postdoctoral fellowship.

Author contributions

Pablo Pinacho: Conceptualization, Investigation, Formal analysis, Writing – original draft, Writing – review & editing. Wenhao Sun: Investigation, Formal analysis, Writing – review & editing. Dan A. Obenchain: Formal analysis, Writing – review & editing. Melanie Schnell: Conceptualization, Funding acquisition, Project administration, Writing – review & editing.

References

[1] H. Oberhammer, *ChemPhysChem*, **2015**, *16*, 282-290.
[2] D. E. Clark, *Chem. Health Saf.*, **2001**, *8*, 12-22.
[3] W. Ando, *Organic Peroxides*, Wiley, Chichester, 1992
[4] W. Adam, *Peroxide Chemistry: Mechanistic and Preparative Aspects of Oxygen Transfer*, Wiley-VCH, Weinheim, 2000.
[5] G. Sienel, R. Rieth, K. T. Rowbottom, *Epoxides. Ullmann's Encyclopedia of Industrial Chemistry*; Wiley-VCH, 2000.
[6] D. W. Gunz, M. R. Hoffmann, *Atmos. Environ.*, **1990**, *24A*, 1601-1633.
[9] S. R. Meshnick, *Int. J. Parasitol*., **2002**, *32*, 1655-1660.
[10] J. Terao, *Cholesterol Hydroperoxides and Their Degradation Mechanism. In Lipid Hydroperoxide-Derived Modification of Biomolecules*, Ed. Y. Kato, Springer, Netherlands, 2014, Vol. 77, pp 83–91.
[11] A. Farkas, E. Passaglia, *J. Am. Chem. Soc.*, **1950**, *72*, 3333-3337.
[12] S. Chubachi, H. Matsui, K. Yamamoto, S. Ishimoto, *Bull. Chem. Soc. Jpn.*, **1969**, *42*, 789-794.
[13] P. A. Giguère, T. K. K. Srinivasan, *J. Mol. Spectrosc*. **1977**, *66*, 168-170.
[17] W. Gordy, R. L. Cook, *Microwave Molecular Spectra*, Wiley-Interscience, New York, 1984.
[18] G. G. Brown, B. C. Dian, K. O. Douglass, S. M. Geyer, S. T. Shipman, B. H. Pate, *Rev. Sci. Instrum.*, **2008**, *79*, 053103.
[19] J. L. Alonso, J. C. López. Microwave spectroscopy of biomolecular building blocks, in *Gas-Phase IR Spectroscopy and Structure of Biological Molecules*, eds: A. Rijs, J. Oomens, Springer, Cham, 2015.
[20] J. T. Hougen, *Can. J. Phys.*, **1984**, *62*, 1392-1402.
[24] M. Fatima, C. Pérez, B. E. Arenas, M. Schnell, A. L. Steber, *Phys. Chem. Chem. Phys.,* **2020**, *22*, 17042–17051.
[25] J. L. Neill, B. J. Harris, A. L. Steber, K. O. Douglass, D. F. Plusquellic, B. H. Pate, *Opt. Express.,* 2013, *21*, 19743.
[26] C. Pérez, A. Krin, A. L. Steber, J. C. López, Z. Kisiel, M. Schnell, *J. Phys. Chem. Lett.*, **2016**, *7*, 154–160.
[27] C. Bannwarth, S. Ehlert and S. Grimme, *J. Chem. Theory Comput.*, **2019**, *15*, 1652–1671.
[28] a) C. Lee, W. Yang, R. G. Parr, *Phys. Rev. B*, **1988**, *37*, 785–789. b) A. D. Becke, *J. Chem. Phys.*, **1993**, *98*, 5648–5652.
[31] Orca Version 5.0. - F. Neese, *WIREs Comput. Mol. Sci.*, **2022**, *12*, e1606.
[32] Gaussian 16, Revision C.01, M. J. Frisch, *et al*., *Gaussian, Inc*., Wallingford CT, 2019.
[33] C. M. Western, *J. Quant. Spectrosc. Radiat. Transf.*, **2017**, *186*, 221-242.
[34] J. K. G. Watson, in *Vibrational Spectra and Structure a Series of Advances*, Vol 6 ed. J. R. Durig, Elsevier, New York, 1977, pp. 1–89.
[35] H. M. Pickett, *J. Mol. Spectrosc.*, **1991**, *148*, 371–377.
[36] Z. Kisiel, PROSPE Programs for ROtational SPEctroscopy, available at http://www.ifpan.edu.pl/~kisiel/prospe.htm; accessed on Sept. 01, 2022.
[37] E. R. Johnson, S. Keinan, P. Mori-Sánchez, J. Contreras-García, A. J. Cohen, W. Yang, *J. Am. Chem. Soc.*, **2010**, *132*, 6498–6506.
[38] J. Contreras-García, E. R. Johnson, S. Keinan, R. Chaudret, J. P. Piquemal, D. N. Beratan, W. Yang, *J. Chem. Theory Comput.*, **2011**, *7*, 625–632.
[39] F. R. Jensen, D. S. Noyce, C. H. Sederholm, A. J. Berlin, *J. Am. Chem. Soc.*, **1960**, *82*, 1256-1257.
[40] S. Blanco, P. Pinacho, J. C. López, *J. Phys. Chem. Lett.*, **2017**, *8*, 6060-6066.
[41] P. Pinacho, S. Blanco, J. C. López, *Phys. Chem. Chem. Phys*, **2019**, *21*, 2177-2185.
[42] M. Juanes, W. Li, L. Spada, L. Evangelisti, A. Lesarri, W. Caminati., *Phys. Chem. Chem. Phys*, **2019**, *21*, 3676-3682.
[43] R. L. Redington, W. B. Olsen, P. C. Cross, *J. Chem. Phys.*, **1962**, *36*, 1311-1326.
[44] C. J. Marsdsen, L. S. Bartell, F. P. Diodati, *J. Mol. Struct.*, **1977**, *39*, 253-262.
[45] R. H. Jackson, *J. Chem. Soc.*, **1962**, 4585-4592.
[46] L. Hedberg, K. Hedberg, P. G. Eller, R. R. Ryan, *Inorg. Chem.*, **1988**, *27*, 232-235.